

Supporting Information

A localized high concentration electrolyte for 4 V-class potassium metal batteries

Wenxin Xu, Huwei Wang, Yueteng Gao, Yaojie Wei, Haodong Zhang, Chongwei Gao, Feiyu Kang*, and Dengyun Zhai*

Experimental Methods

Materials: Potassium bis(fluorosulfonyl)imide (KFSI) (>99.9%, Fluolyte) was dried under vacuum at 90 °C for 24 hours before use. 0.5 M KPF₆ EC DEC (volume ratio = 1:1) was purchased from Ltd. Diethylene glycol dimethyl ether (DEGDME) (>99%, Sigma-Aldrich) and TFETFE (>99%, Sigma-Aldrich) were stored over 4 Å molecular sieves (Sigma-Aldrich).

Preparation of the PB Electrode: Prussian blue power was synthesized according to a modified co-precipitation method.¹ Concretely, potassium citrate (4 g) and FeCl₂ (0.8 g) were dissolved into deionized water (100 mL) under nitrogen atmosphere followed by adding potassium ferrocyanide aqueous solution (3 mmol) dropwise with vigorous stirring. After stirring the solution for 10 hours and centrifugal treatment, the precipitation was vacuum-dried overnight under 120 °C. Then the Prussian blue cathode was prepared by mixing the KPB powder, carbon black (Sinopharm Chemical Reagent Co., Ltd) and polyvinylidene difluoride binder (PVDF, Canrd) at a weight ratio of 7:2:1. Stirring the mixture with N-methylpyrrolidone (AR, Sinopharm Chemical Reagent Co., Ltd) for 6 hours to form uniform slurry followed by pasting it on an Al foil (MTI) and dried in a vacuum oven at 110 °C for 12 hours. After drying, the coated foil was cut into circular pieces with the diameter of 12 mm. The average mass loading is ~0.8 mg cm⁻².

The K metal chunk (>98%, Sigma-Aldrich) was pressed into circular sheet (with a diameter of 13 mm and thickness of ~ 150 μm) and placed on stainless steel sheet. K | PB cells were assembled with PB as the cathode and K metal as anode. K | Cu half cells were consisted of K metal as the counter electrode and Cu foil (diameter of 14 mm) as the working electrode. The applied separator was a piece of Celgard 2320 (polypropylene-polyethylene-polypropylene, 25 μm thickness) and a piece of glass fiber (GF/A, Whatman). 100 μL electrolytes were added into each CR 2032 typed cell. All the cells were assembled in an argon filled glove box with oxygen and water contents below 0.1 ppm.

Electrochemical measurements: The galvanostatic discharge/charge tests of K | PB and K | Cu coin cells were conducted on a standard eight-channel battery test (CT2001A, Wuhan LAND Electronics Co., Ltd.) at 25 °C. For K | Cu cells, the current density of charge and discharge was 0.25 mA cm⁻². And the charge cutoff voltage of K | Cu cell was 1.0 V (vs. K⁺/K). The CE was calculated as the K stripping capacity divided by the K plating capacity during a single cycle. The discharge and charge cutoff voltages of K|PB cell was 2.5 V and 4.3 V, 4.4 V (vs. K⁺/K). 1 C = 100 mA/g. LSV measurements were conducted on a Solartron workstation with K | Al coin cells using Al as working electrode and K metal as counter electrode. CV studies of

the electrolytes were conducted with CR 2032 coin cells using PB as a working electrode and K metal as a counter electrode on a VMP 3 workstation. Both LSV and CV were carried out at a scan rate of 0.5 mV s⁻¹.

Materials characterization: Raman spectra were performed on HORIBA HR800 spectrometer (633-nm Ar-ion laser) with the electrolytes storing in cuvettes. Ionic conductivities were measured on a FE38-Standard conductivity meter (Mettler Toledo, Switzerland) at 25 °C. Electrolyte viscosity measurements were carried out with a Brookfield DV2⁺ Pro Viscometer. Morphological observation was conducted on a scanning electron microscopy (SEM, HITACHI SU8010, Japan). X-ray photoelectron spectroscopy (XPS) analysis was obtained on a PHI 5000 VersaProbe II (Ulvac-Phi, Japan) spectrometer with monochromatic Al-K α X-ray source. The obtained XPS data was calibrated with respect to the C-C speak at 284.8 eV in C1s spectrum. For SEM, K metal with 4 mAh cm⁻² was deposited on the Cu substrate for further characterization. All coin cells were disassembled in the argon glove box to obtain the samples for SEM and XPS characterizations. The potassium electrodes to be characterized were washed by solvent of DEGDME followed by DME for several time and then transported from the argon-filled glove box to characterization instruments in an air-free transfer vessel. Electrochemical impedance spectroscopy (EIS) was conducted using a Solartron workstation, with a frequency range of 100 KHz to 100 mHz and an AC voltage amplitude of 10 mV.

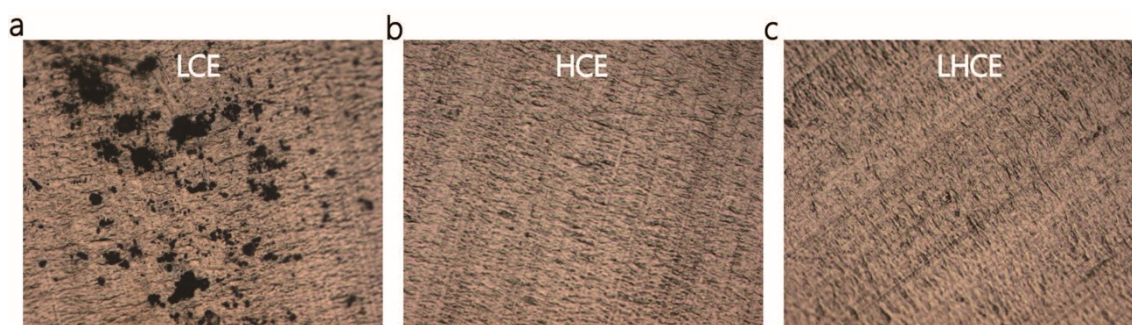


Fig. S1. Optical microscopy images (200x) of the Al current collector after the LSV of (a) LCE (b) HCE and (c) LHCE.

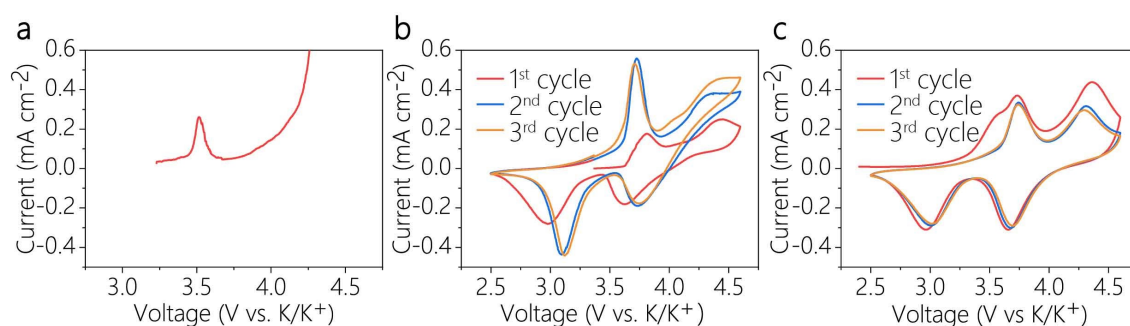


Fig. S2. CV curves of (a) LCE, (b) HCE and (c) LHCE with PB cathodes as working electrodes in K | PB coin cells.

For the LCE, only first K^+ de-intercalation at 3.5 V can be observed and then the electrolyte suffers a continuous oxidative decomposition. But for the HCE and the LHCE, CV profiles depict two oxidation peaks around 3.7 and 4.2 V, consistent with the reported results.¹

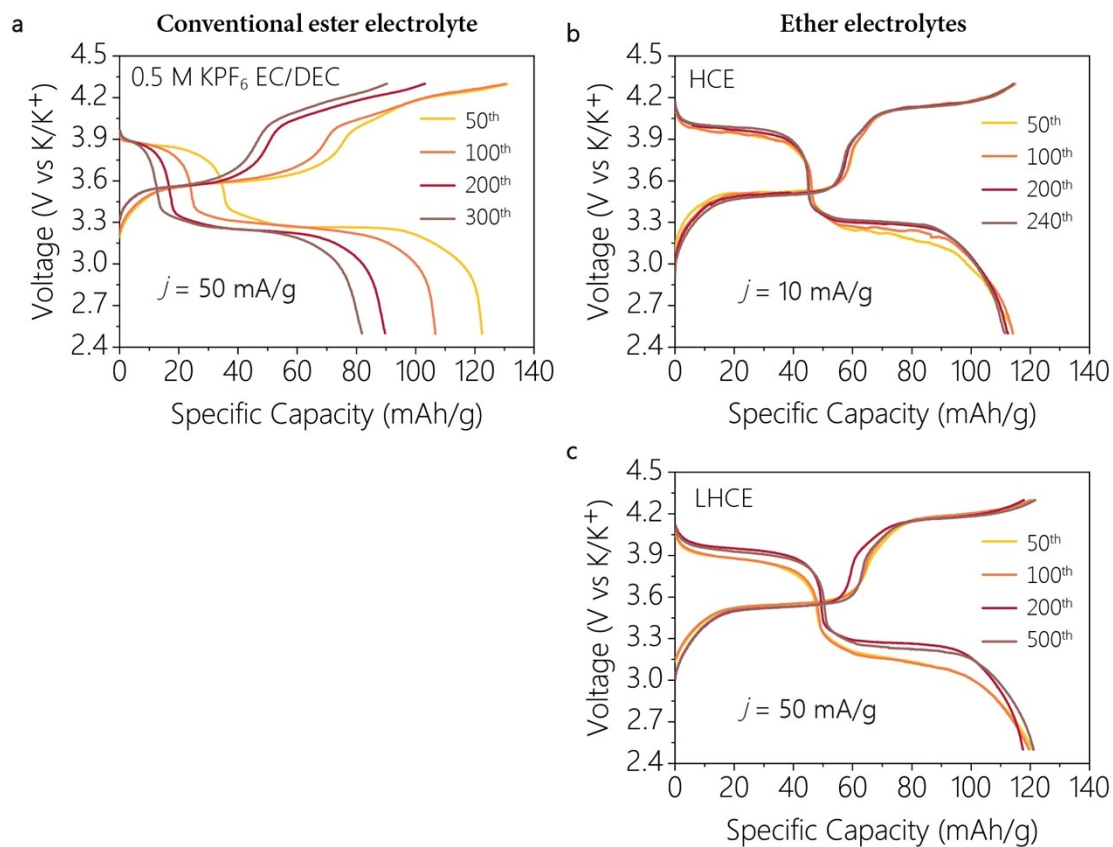


Fig. S3. Voltage profiles of K | PB cells in (a) 0.5 M KPF_6 EC DEC electrolyte at 50 mA g^{-1} , (b) HCE at 10 mA g^{-1} and (c) LHCE at 50 mA g^{-1} .

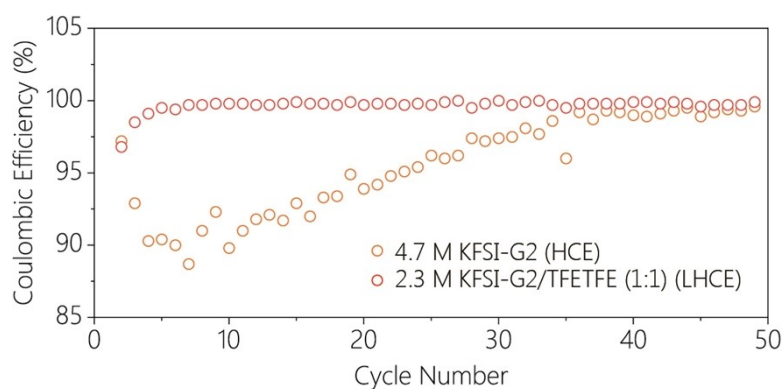


Fig. S4. Coulombic efficiency of K | PB coin cells in 4.7 M HCE and 2.3 M LHCE during the initial 50 cycles.

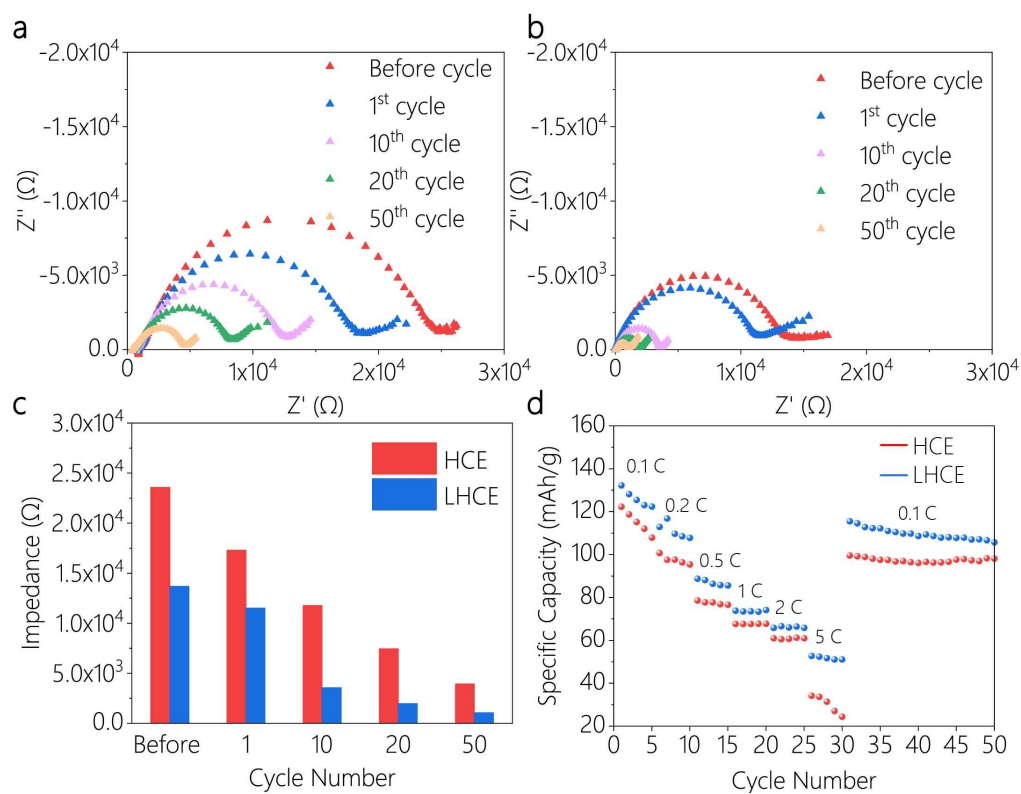


Fig. S5. Nyquist plots of K | PB batteries with (a) HCE and (b) LHCE before and during different cycles. (c) The comparison of interfacial resistance between HCE and LHCE. (d) The rate performance of K | PB batteries in HCE and LHCE. 1 C=100 mA g⁻¹.

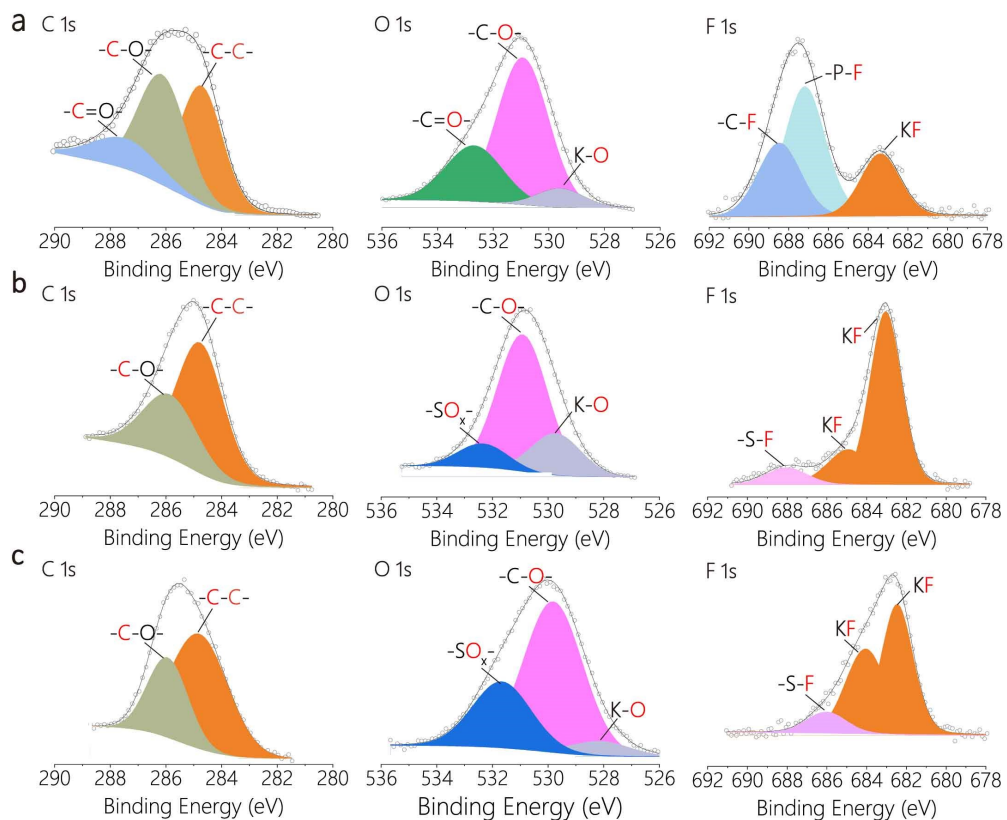


Fig. S6. XPS chemical analysis of SEI for C 1s, O 1s and F 1s in (a) 0.5 M KPF₆ EC/DEC, (b) HCE and (c) LHCE.

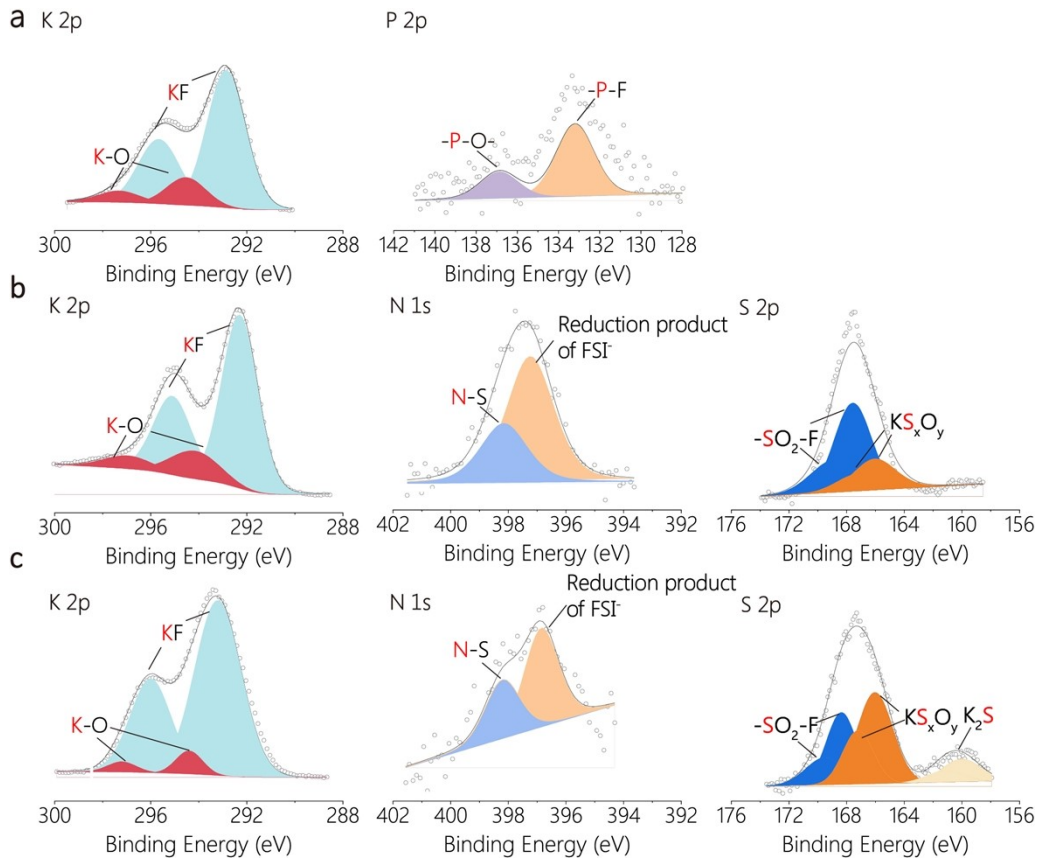


Fig. S7. XPS chemical analysis of SEI for (a) P 2p and K 2p in 0.5 M KPF₆ EC/DEC. XPS chemical analysis of SEI layers for N 1s, S 2p and K 2p in (b) HCE and (c) LHCE.

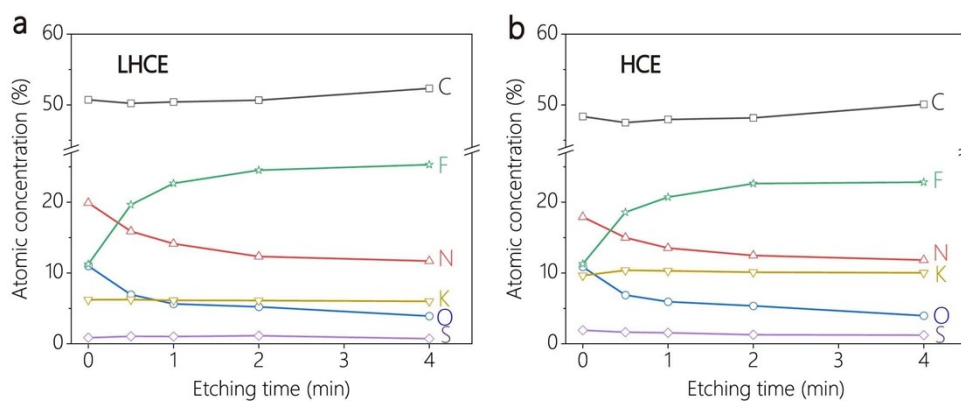


Fig. S8. Quantified atomic composition ratios of the cathode electrolyte interphase obtained by XPS spectra for the PB cathodes cycled in (a) LHCE and (b) HCE.

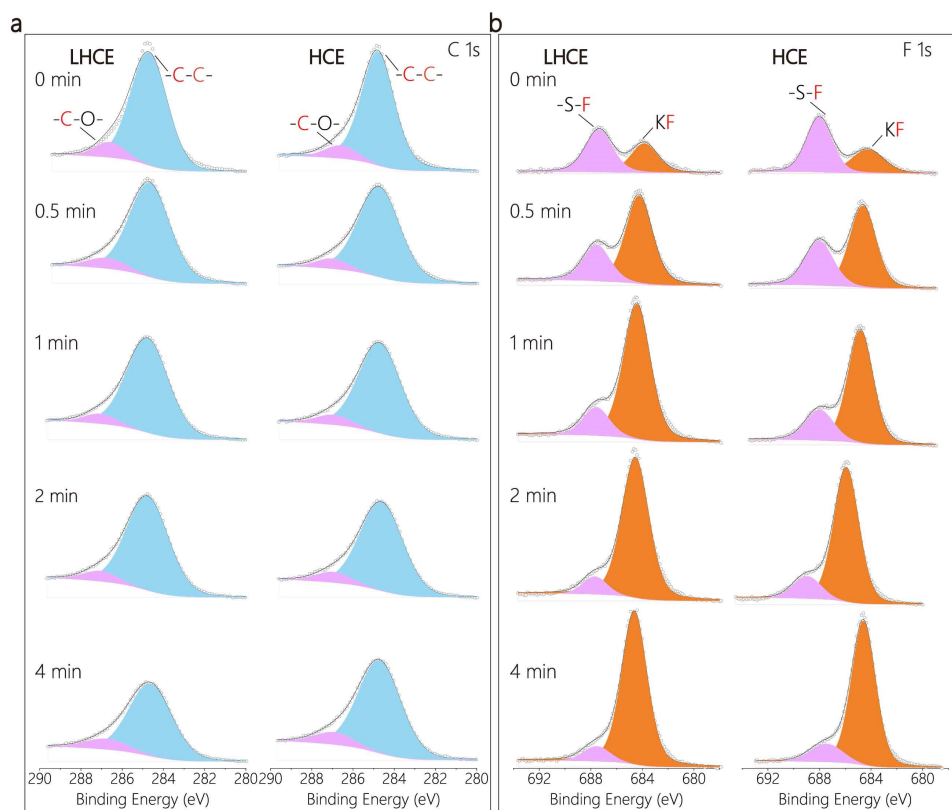


Fig. S9. (a) C 1s and (b) F 1s spectra of the surface film on PB cathode at different etching time after cycles in the ether-based HCE and LHCE.

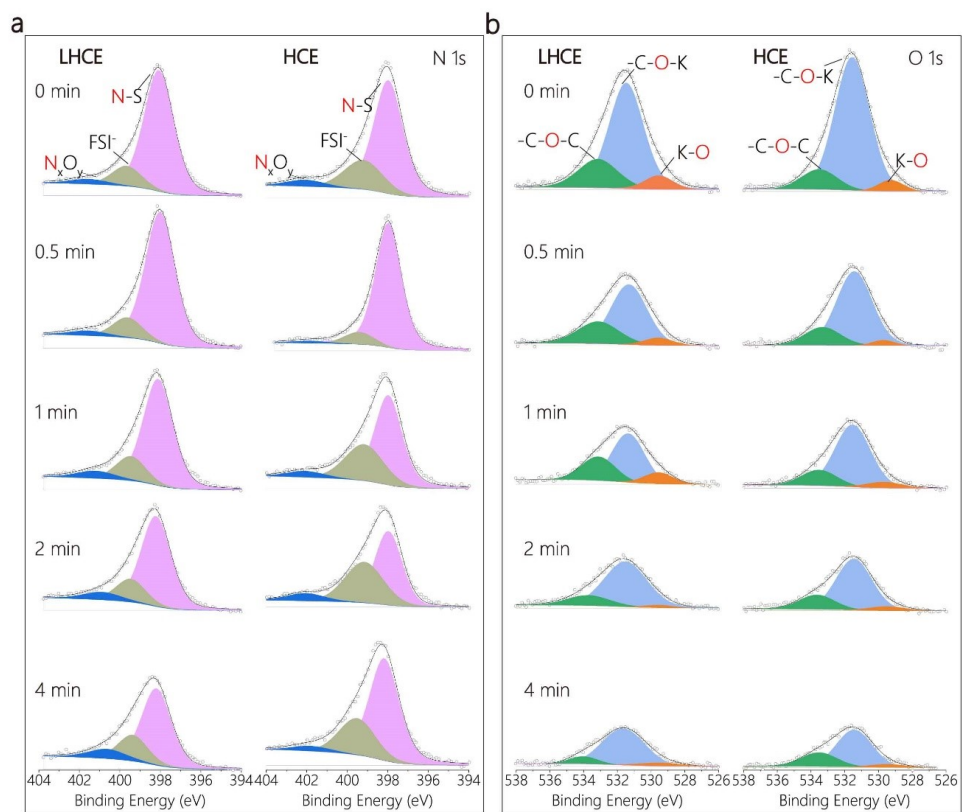


Fig. S10. (a) N 1s and (b) O 1s spectra of the surface film on PB cathode at different etching time after cycles in the ether-based HCE and LHCE.

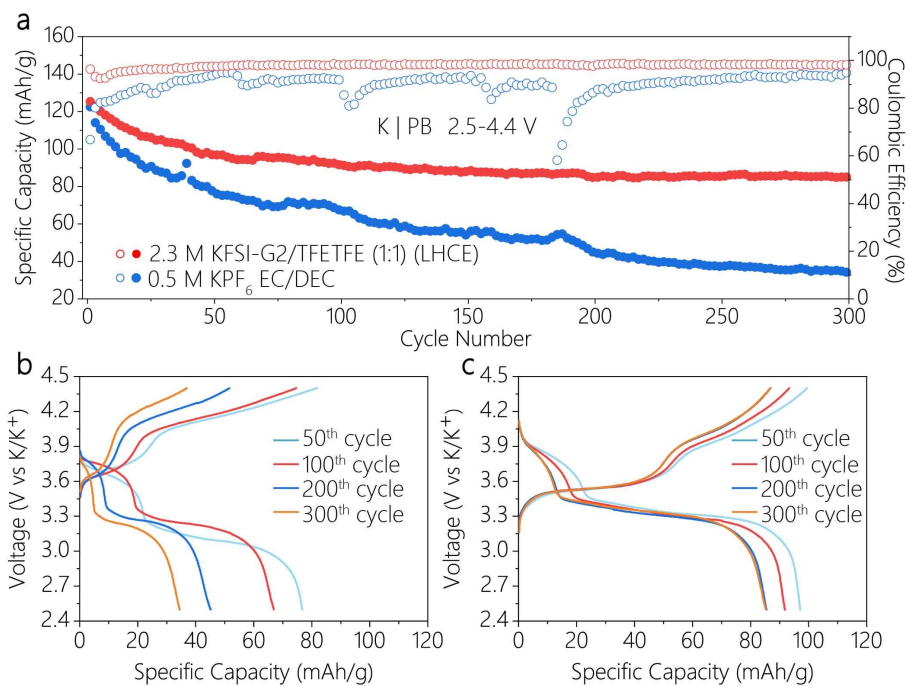


Fig. S11. (a) Cycling performance of K | PB batteries under the cut-off voltage of 4.4 V. The voltage profiles of K | PB batteries in (b) 0.5 M KPF₆ EC DEC and (c) LHCE under the cutoff voltage of 4.4 V.

References

- [1] G. He, L. F. Nazar, *ACS Energy Letter*. **2017**, 2, 1122.